Figures and figure supplements

Functional role of the type 1 pilus rod structure in mediating host-pathogen interactions

Caitlin N Spaulding *et al*

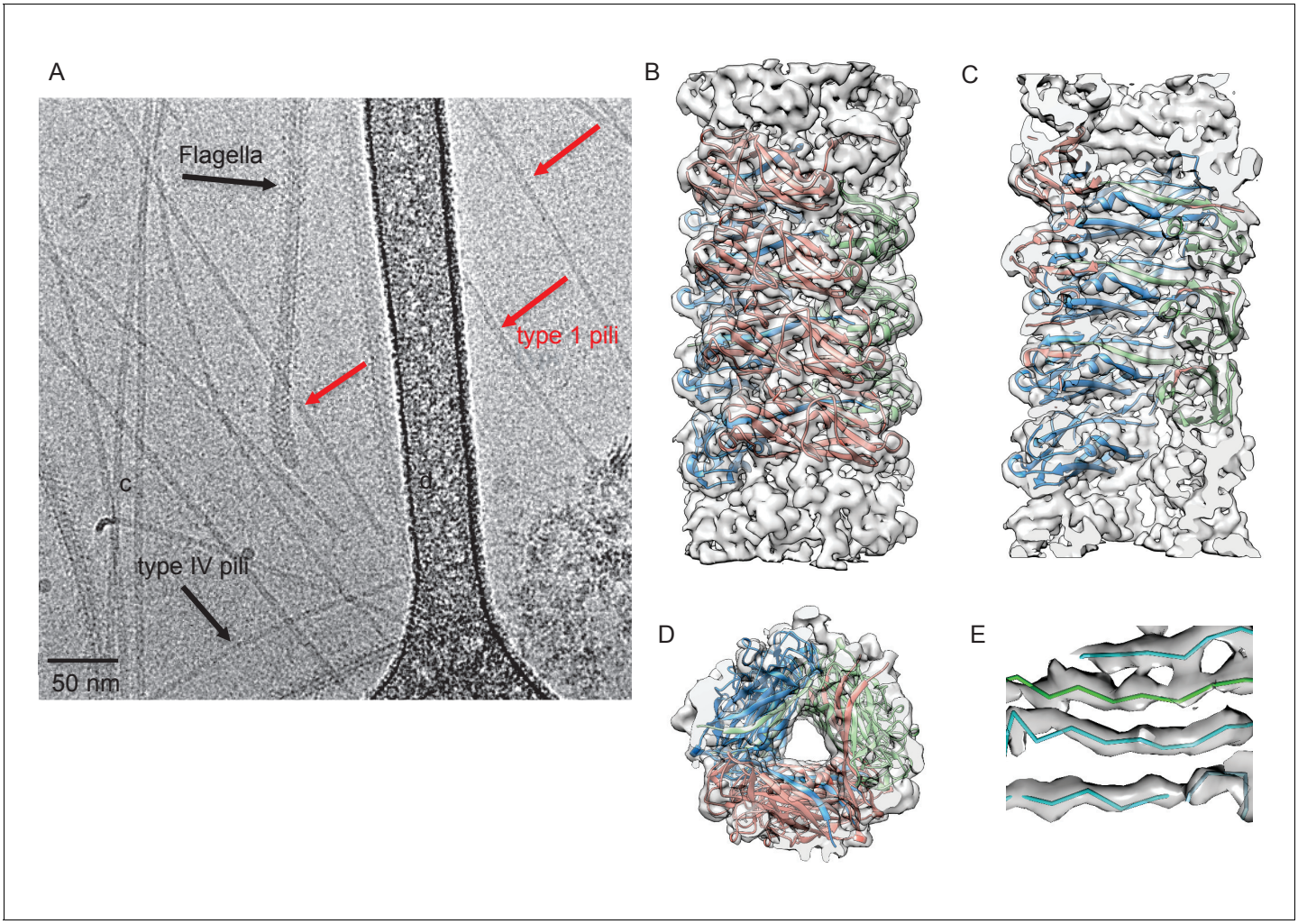

Figure 1. Cryo-EM Structure of Type 1 pili. (**A**) An electron micrograph of type 1 pili in vitreous ice, surrounded by type 4 pili and flagellar filaments. (**B**) Side view, (**C**) interior view (the front half of the reconstruction has been removed) and (**D**) top view of overall reconstruction of FimA rod with subunits along the same left-handed 3-start helix colored in either blue, salmon or green. (**E**) Close-up view of donor strand complementation (DSC) in the central lumen showing that the β-strands in the reconstruction are very well resolved.

DOI: https://doi.org/10.7554/eLife.31662.003

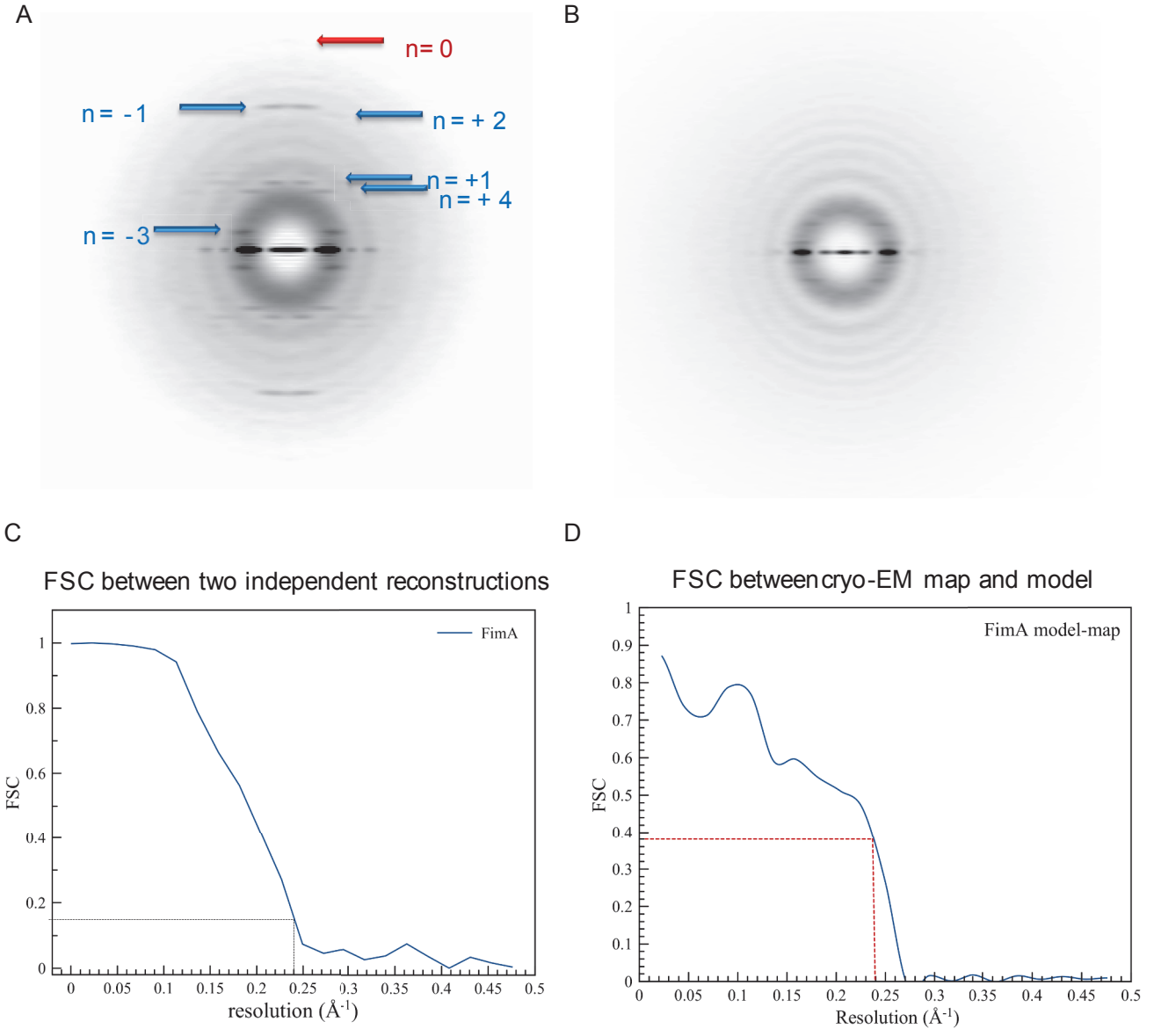

Figure 1—figure supplement 1. Details of cryo-EM reconstruction of type 1 pili. (**A**) Averaged power spectrum from the segments of type 1 pili, which shows the meridional at ~1/(7.5 Å) indicated by the red arrow. The blue arrow indicates layer lines containing Bessel orders + 1,+2,+4,–1, and −3. (**B**) The power spectrum for the Type IV pili in the same preparation. (**C**) FSC plot generated from two independent half maps, each reconstructed from two independent dataset, shows a resolution of ~4.2 Å at FSC = 0.143. (**D**) FSC plot generated from the comparison of the cryo-EM map with the atomic model shows a resolution of ~4.2 Å at FSC = 0.38 (=$0.143^{1/2}$).

DOI: https://doi.org/10.7554/eLife.31662.004

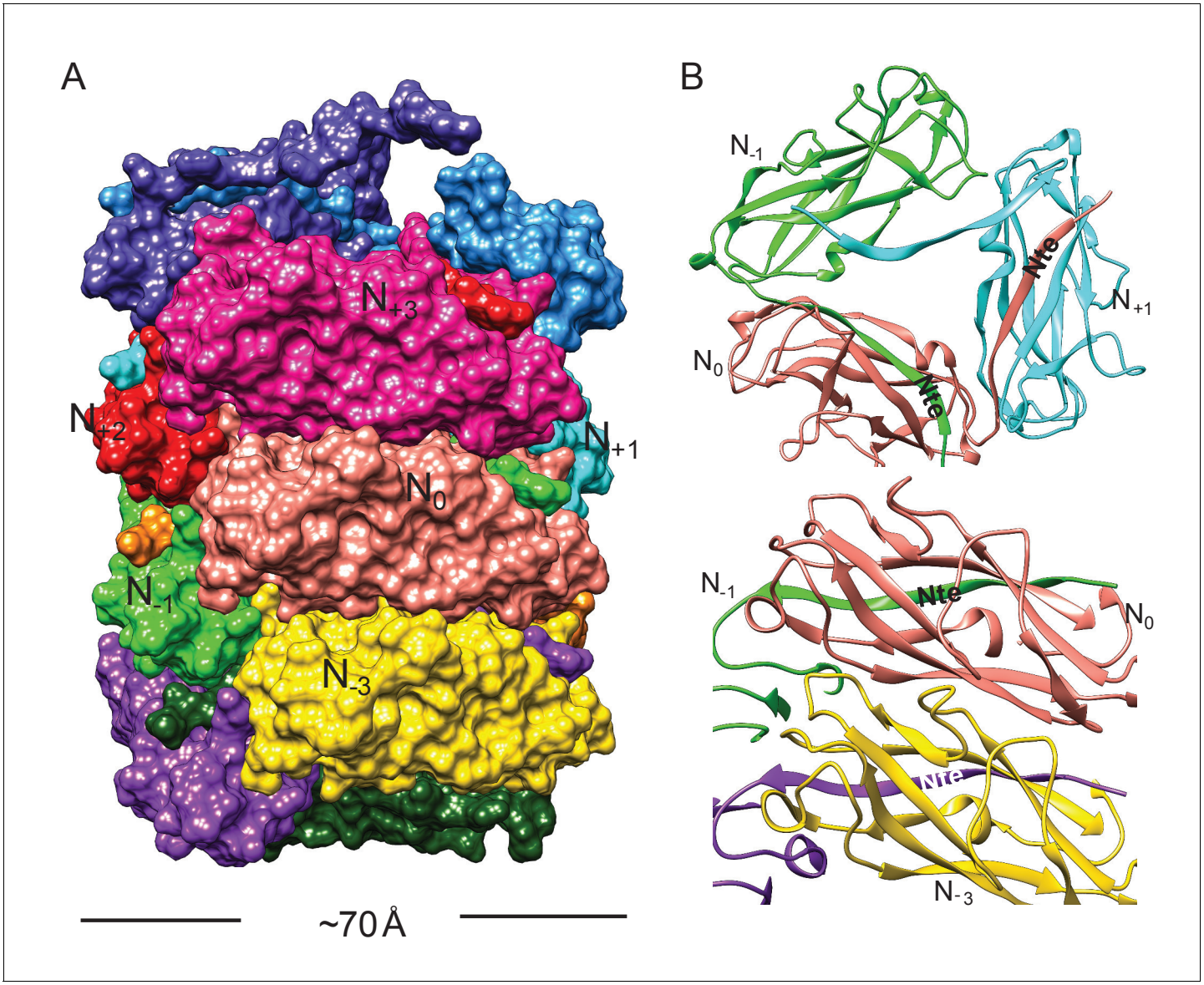

Figure 2. Subunit interface of the FimA rod. (**A**) Surface view of FimA rod model with subunits numbered along the right-handed 1-start helix. Each subunit is in a different color. (**B**) Ribbon representation to illustrate the interface of subunit N_0 (in salmon) with neighboring subunits.

DOI: https://doi.org/10.7554/eLife.31662.005

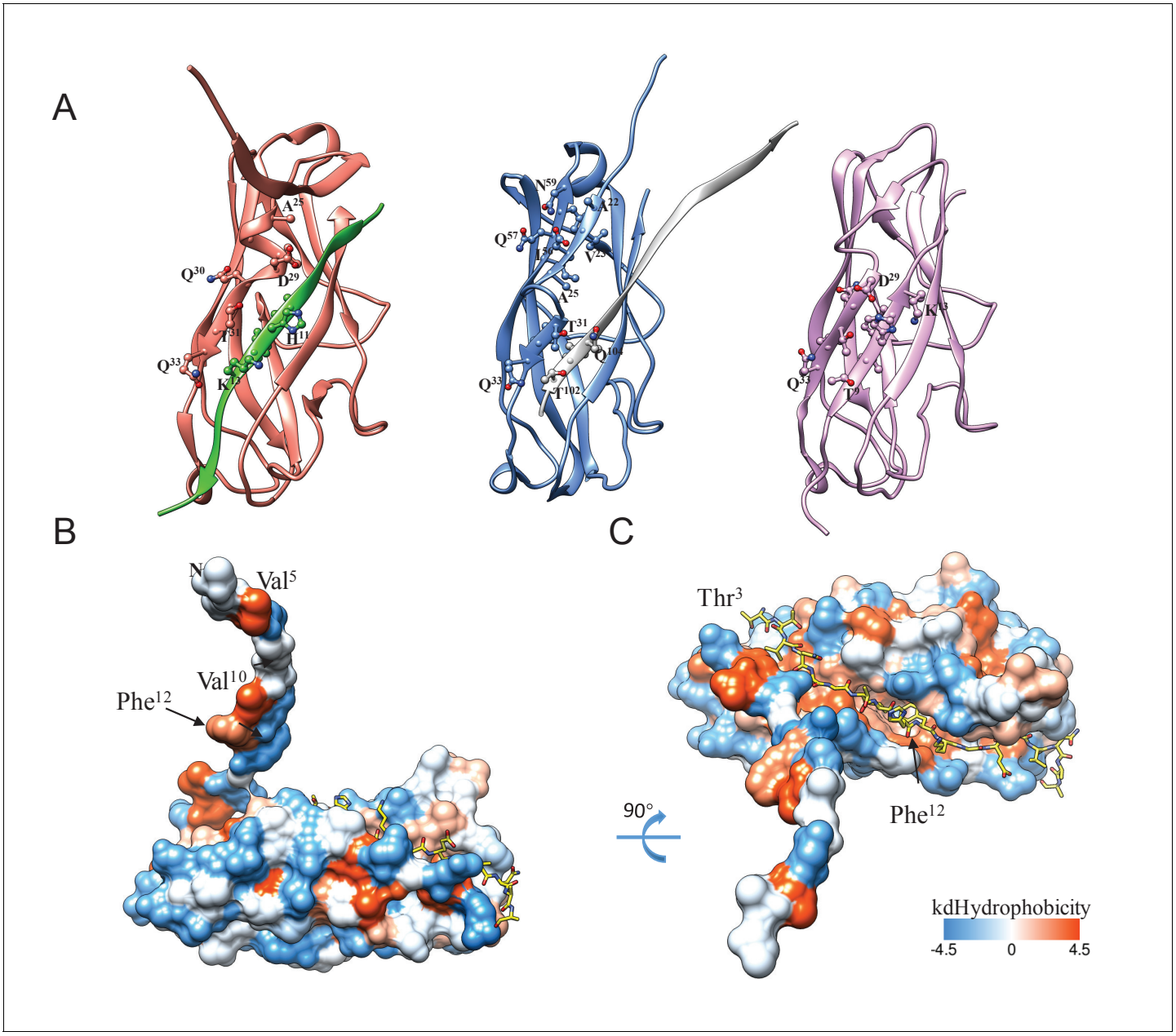

Figure 2—figure supplement 1. Nte inserts into the hydrophobic groove of the neighboring subunit. (**A**) Comparison of the DSC within the helical rod, within the FimA:FimC complex (PDB ID:3SQB), and in the self-complemented FimA monomer (PDB ID:2M5G). FimA in the helical rod is shown in salmon and Nte from the adjacent subunit is shown in green; FimA in FimA:FimC complex is shown in blue and FimC donor strand is shown in grey; FimA self-complemented monomer is shown in plum. (**B,C**) FimA rod subunit surface is colored according to hydrophobicity, with the adjacent subunit's Nte shown in a stick representation. Phe12 sits in a large hydrophobic pocket of the adjacent subunit.

DOI: https://doi.org/10.7554/eLife.31662.006

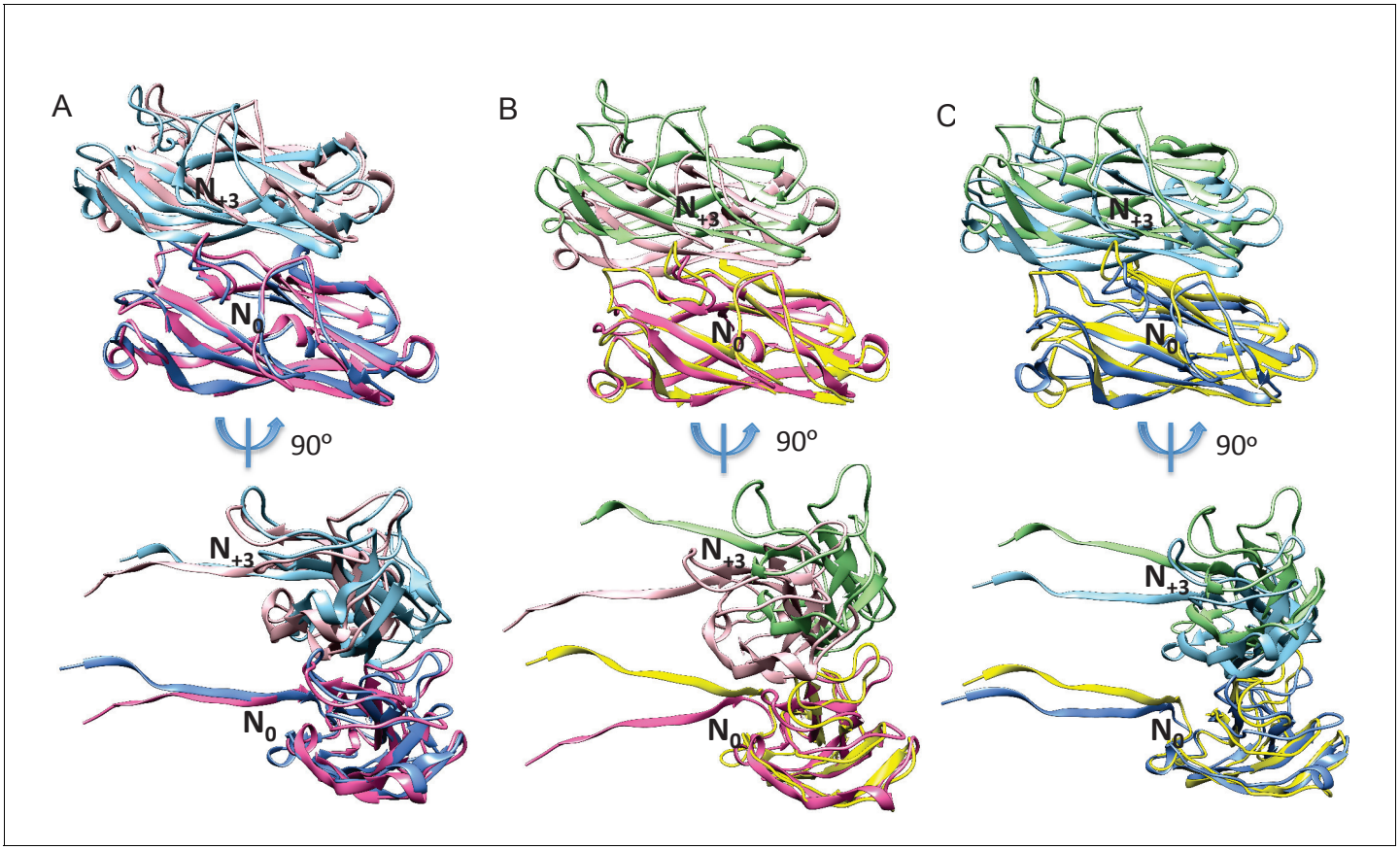

Figure 2—figure supplement 2. Comparison of subunit N_0 and N_{+3} interfaces with previously deposited FimA pilus rod models. (**A**) Our FimA pilus rod model and the deposited solid-state NMR FimA model 2N7H, when aligned with their N_0 subunit have an overall RMSD of 5.7 Å for subunits N_{+3}. (**B**) Our FimA pilus rod model and solid-state NMR FimA model 2MX3 when aligned with subunit N_0 have an overall RMSD of 11.0 Å for subunits N_{+3}. (**C**) FimA models 2N7H and 2MX3 when aligned with their N_0 subunit, the overall RMSD is 5.6 Å for subunit N_{+3}. The N_0 and N_{+3} subunits of our FimA model are colored in hot pink and pink, respectively. The N_0 and N_{+3} subunits of 2N7H are colored in dodger blue and light blue, respectively. The N_0 and N_{+3} subunits of 2MX3 are colored in yellow and green, respectively.

DOI: https://doi.org/10.7554/eLife.31662.007

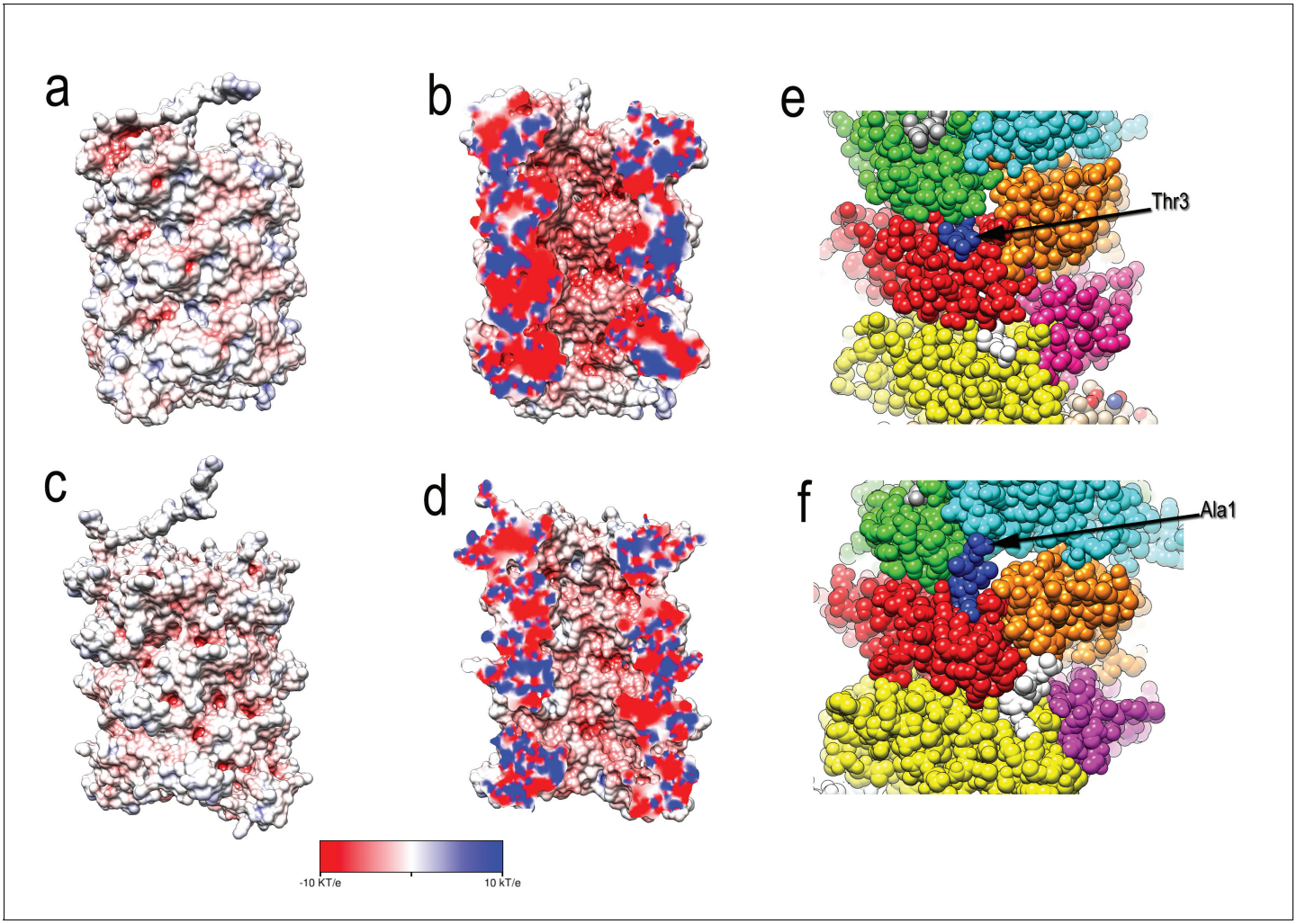

Figure 2—figure supplement 3. Comparison of type 1 pili and P pili. (**A**) The exterior and (**B**) central lumen of type 1 pili colored according to the electrostatic potential. (**C**) The exterior and (**D**) central lumen of P pili (PDB ID: 5FLU) colored according to the electrostatic potential. Red corresponds to a potential of −10 kT/e, and blue corresponds to a potential of 10 kT/e. (**E, F**) structures of type 1 and P pilus rods with each FimA subunit shown in a different color. (**E**) The N-terminus of FimA in the type 1 pilus projects out of the structure and makes no contacts with other subunits. (**F**) In contrast, the N-terminus in P pili (PDB 5FLU) forms a 'staple' which involves contacts with two other subunits.

DOI: https://doi.org/10.7554/eLife.31662.008

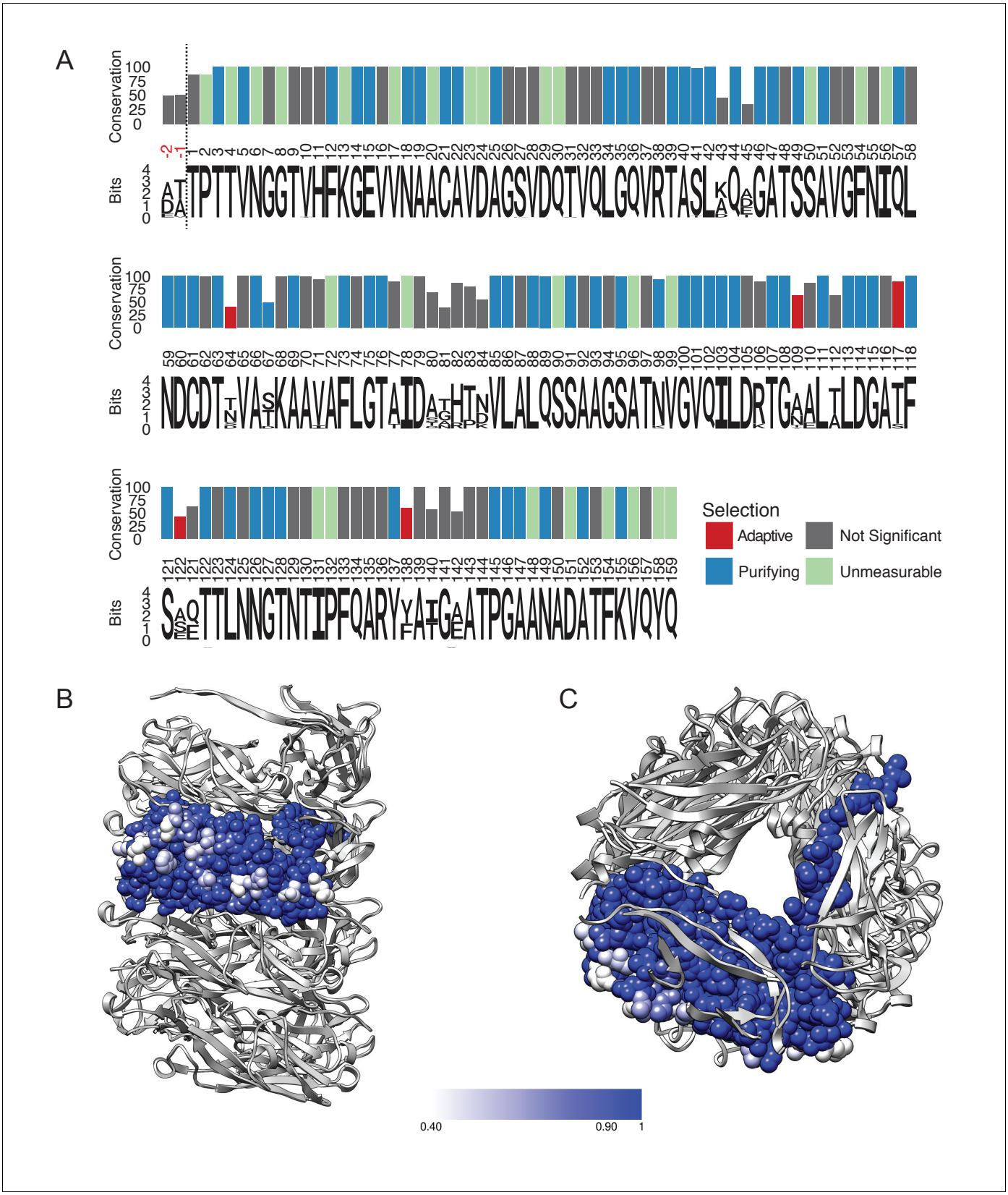

Figure 3. FimA conservation and variability. (**A**) Conservation, consensus amino acid identity, and selection pressures on residues within the mature form of the FimA protein measured by alignment of 1,828 sequences. Numbering here is based on FimA from BW25113 and the vertical dashed line

Figure 3 continued on next page

Figure 3 continued

indicates the location of the two amino acid residues, in red, that are present in some FimA sequences. Consensus amino acid residues are shown at each position. Height of the residues corresponds to their information content (bits) where the larger size indicates greater certainty that residue shown is the consensus residue at that position. The vertical bars represent the proportion of strains with the consensus amino acid (0–100%). Vertical bars are colored by selection pressure acting upon the amino acid position, with red and blue bars indicating residues with codons under adaptive and purifying selection, respectively, as measured by a χ^2 (chi-squared) test. Green bars indicate codons with too little variability for evolutionary analysis and grey indicates amino acid positions that do not show statistically significant evidence for selection. (**B,C**) The degree of conservation for every FimA residue shown in (**A**) has been mapped onto a single subunit in our rod model. The absolutely conserved residues are in blue, the residues that are 40% conserved (the greatest degree of variability found) are in white, and light blue represents 90% conservation. Every residue facing the lumen is 100% conserved. Overall, FimA displays strong signals of purifying selection resulting in conservation with hotspots of adaptive selection resulting in variability of surface residues.

DOI: https://doi.org/10.7554/eLife.31662.009

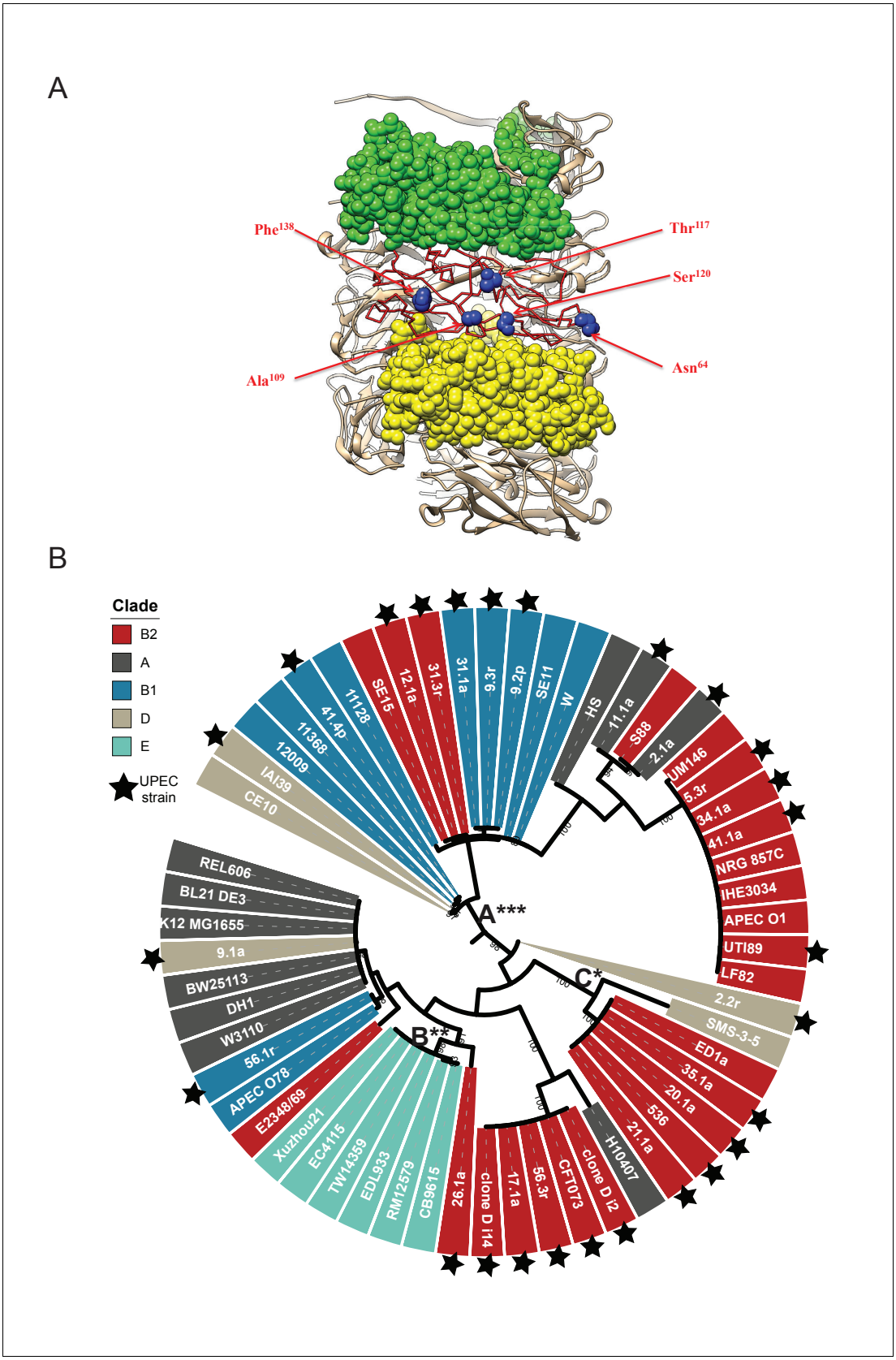

Figure 3—figure supplement 1. Location of FimA residues under positive selection for change in the helical rod. (**A**) Five residues in $FimA_{BW25113}$, Asn64, Ala109, Thr117, Ser120 and Phe138, under adaptive selection are all located on the outside of the pilus rod and are shown in blue spheres. (**B**)

Figure 3—figure supplement 1 continued on next page

Figure 3—figure supplement 1 continued

Phylogenetic analysis of the carriage and evolution of the *fimA* gene in a curated dataset of *E. coli* genomes. A total of 57 *fimA* sequences were aligned and used to construct a phylogenetic tree with bootstrap support (between 80% and 100%) indicated along internal branches. Taxon labels are colored according to their clade of origin and UPEC strains are indicated with a star. Measurement of the rates of non-synonymous (*dN*) to synonymous (*dS*) mutation for each branch identified three branches carrying many sequences from UPEC strains are under episodic, diversifying selection (labeled A, B, and C). Statistical significance for these measures are indicated by asterisks, with *$p \leq 0.05$, **$p \leq 0.01$, and ***$p < 0.001$ by likelihood ratio χ^2 (chi-squared) test.

DOI: https://doi.org/10.7554/eLife.31662.010

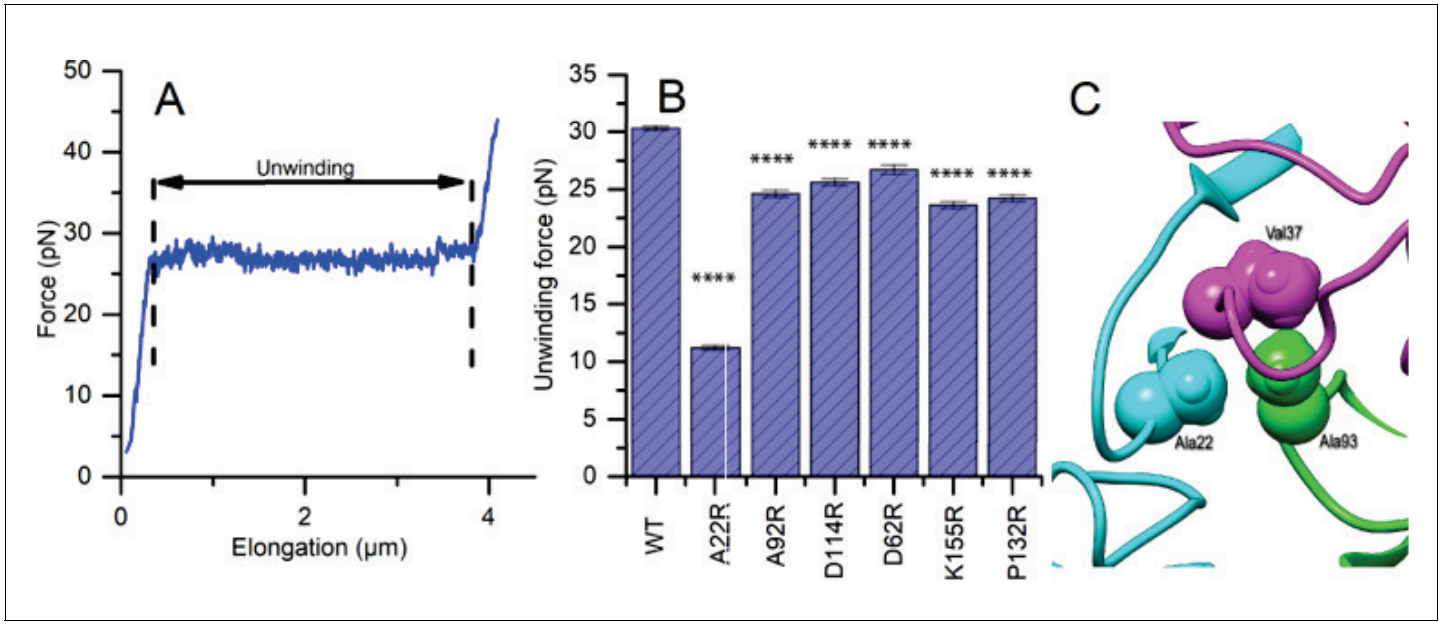

Figure 4. Mutations to FimA alter the force required to unwind the pilus. (**A**) Force response of a single type 1 pilus. The force response is composed of three phases, elastic stretching of the shaft, unwinding of the shaft, and elastic stretching of individual subunits in an open coil. (**B**) Bar chart showing the average unwinding force of $FimA_{BW254113}$ wildtype (WT) and mutants expressed in trans in UTI89-LONΔ*fimA* (**C**) Ala22 (cyan) plays an important role in the inter-subunit contacts through interacting with Val37 (magenta) from a second subunit and Ala93 (green) from a third subunit. (**B**) Bar chart showing the average unwinding force of measured pili where the error bars represent the standard error of the mean [WT, 30.3 ± 0.2 pN, N = 13, 2 replicates; A22R, 11.2 ± 0.2 pN, N = 25, 2 replicates; A92R, 24.6 ± 0.3 pN, N = 19, 2 replicates; D114R, 25.6 ± 0.3 pN, N = 16, 2 replicates; D62R, 26.7 ± 0.4 pN, N = 16, 2 replicates; K155R, 23.6 ± 0.3 pN, N = 14, 2 replicates; P132R, 24.1 ± 0.3 pN, N = 15, 2 replicates]. All replicates biological. ****p<0.0001 by unpaired, two-sided t-test).

DOI: https://doi.org/10.7554/eLife.31662.011

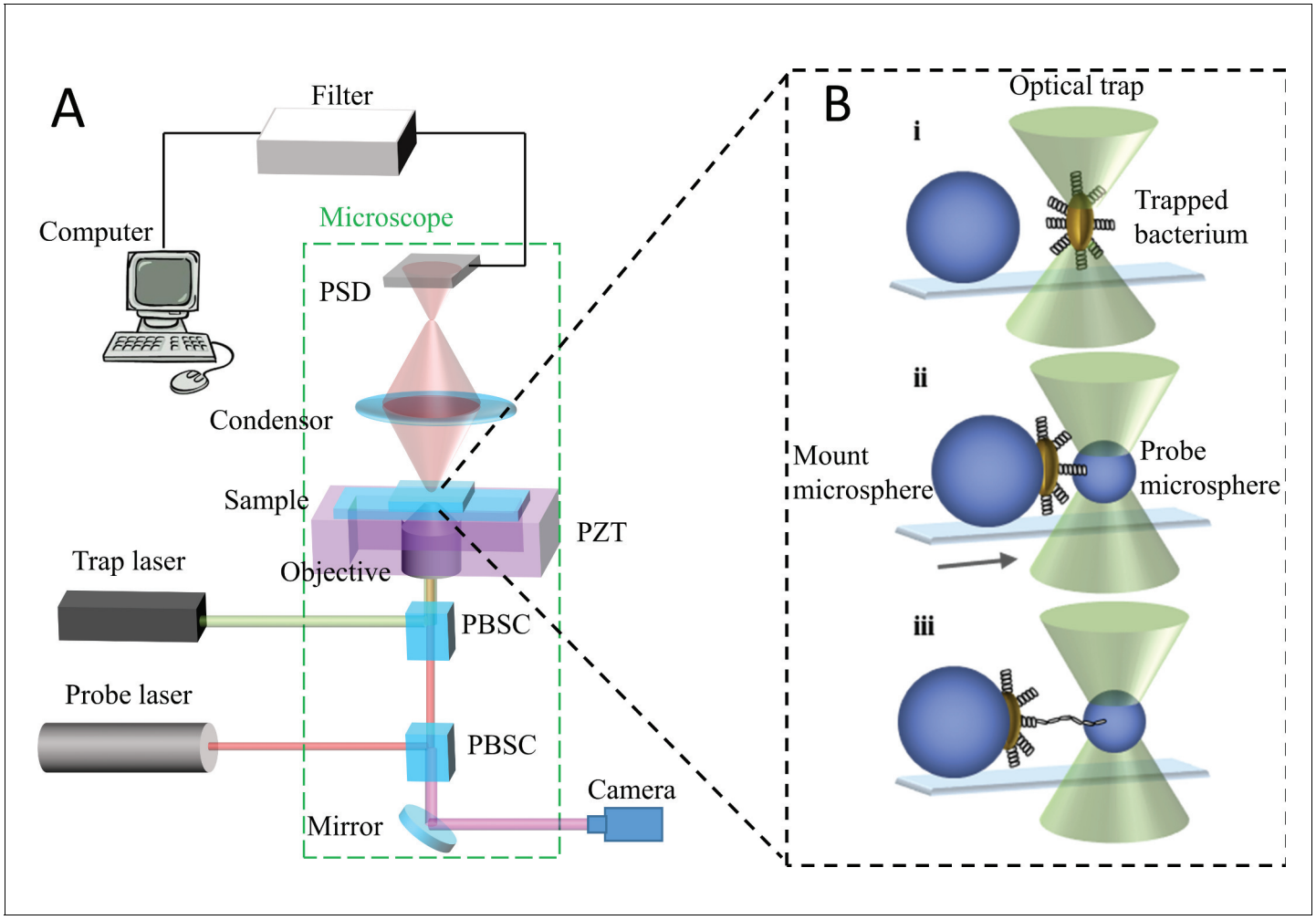

Figure 4—figure supplement 1. Schematic illustration of the optical tweezer setup. (**A**) The trap and probe laser beams are merged using a polarizing beam splitter cube (PBSC) positioned inside the microscope. The two laser beams are thereafter focused by the objective inside the sample chamber. The weak probe laser beam (μW), refracted by the object and collected by the condenser, is illuminating a PSD-detector that converts the incoming light to a photocurrent, which in turn is converted to a voltage signal. (**B**) Schematic illustration of a force spectroscopy experiment. A single cell or probe microsphere can be trapped by the laser. (i) A single bacterium is mounted onto a large immobilized microsphere. (ii) A probe microsphere is trapped and brought into contact with bacterial pili. iii) The bacterium and trapped microsphere are separated and an attached pilus is unwound.
DOI: https://doi.org/10.7554/eLife.31662.012

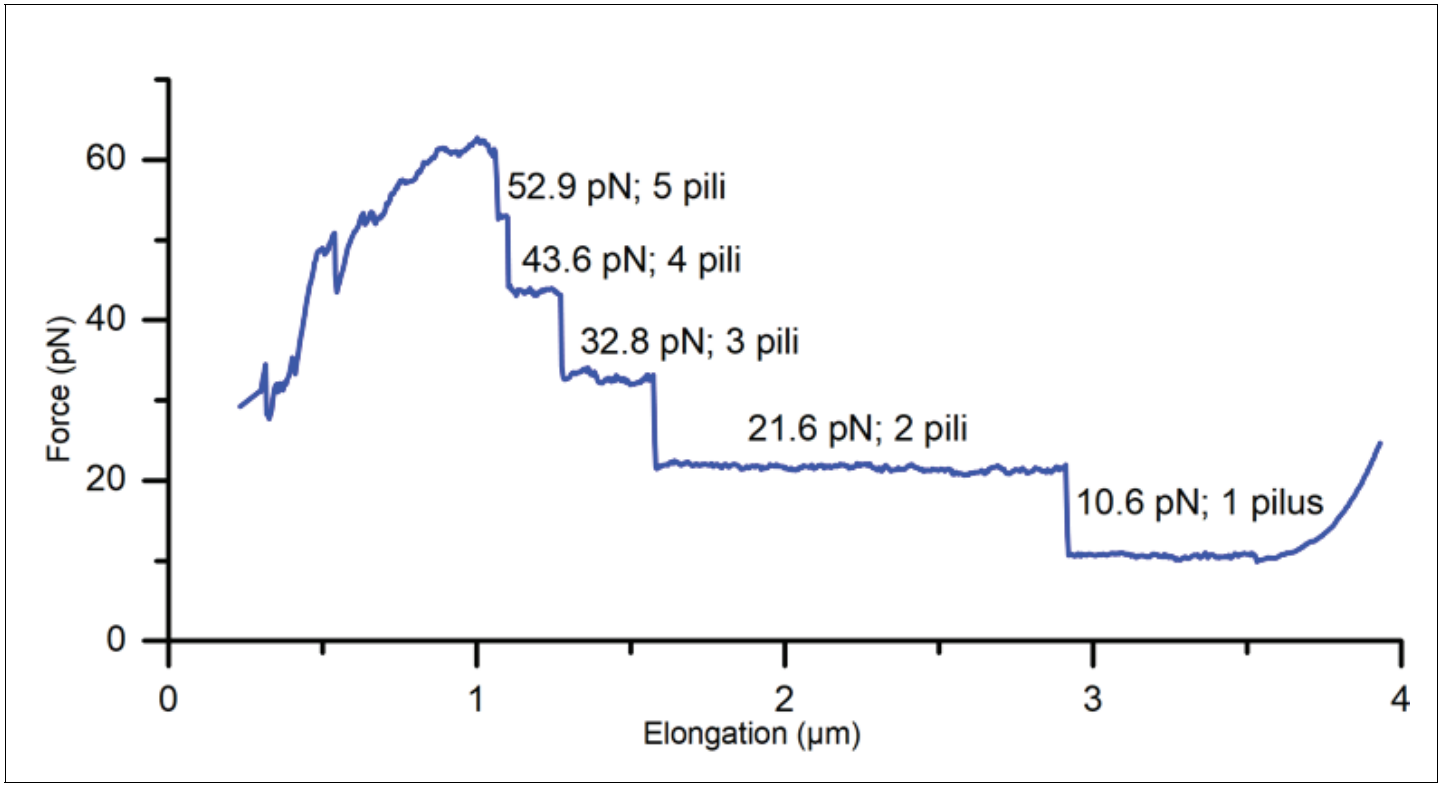

Figure 4—figure supplement 2. Force spectroscopy measurement showing attachment of multiple pili (A22R). Since the uncoiling force of a pilus being extended by a attached microsphere is constant, the measured force response of all attached pili is a multiple of the force required to uncoil a single pilus, thus providing discrete values for each force plateau.

DOI: https://doi.org/10.7554/eLife.31662.013

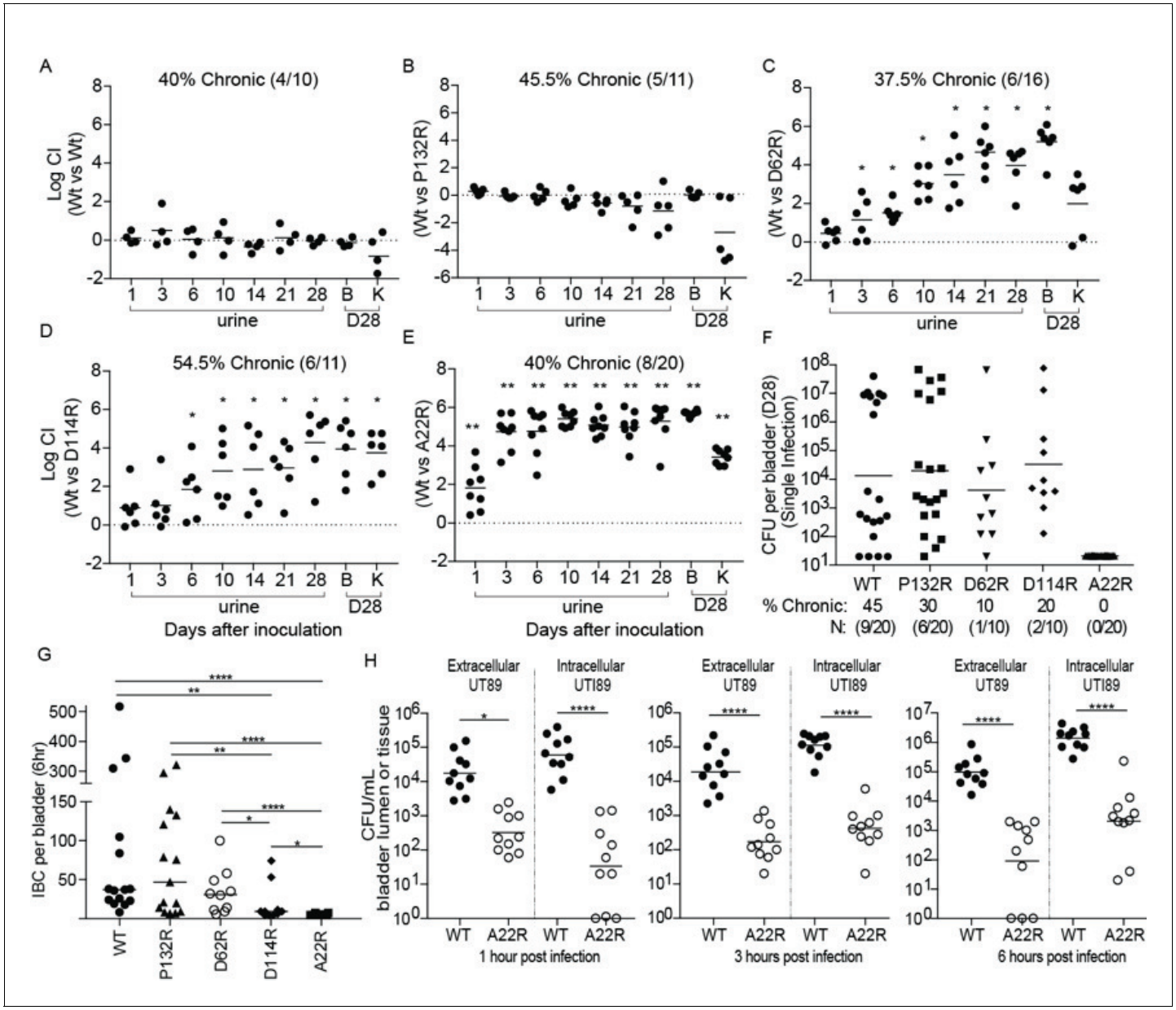

Figure 5. Point mutations in FimA alter UPEC pathogenesis in the bladder. C3H/HeN mice were concurrently transurethrally inoculated with 1×10^8 CFU of wildtype (WT) UTI89 and one of four isogenic UTI89 strains containing point mutations in the *fimA* gene. (**A–E**) Longitudinal urinalyses were performed over 28 days and examination of UTI89 and FimA mutant titers in bladders and kidneys were determined at time of sacrifice (28 dpi). (**F**) Mice were also infected singly, via transurethral inoculation, with UTI89 or FimA mutant strains. Longitudinal urinalysis was perfomed over 28 days (***Figure 5—figure supplement 3***). Bladders titers taken at 28 dpi after single infections are shown in panel F along with the percentage of mice that developed chronic UTI (% chronic) along with the number of mice used in the study (**N**). (**G**) Number of intracellular bacterial communities (IBCs) formed by indicated strain at 6 hr post infection (hpi). (**H**) Mice were singly infected with WT or A22R mutant and the ability of each strain to invade into bladder tissue was assed as 1, 3, and 6 hr post infection. Intracellular bacteria were able to invade into the bladder tissue while extracellular bacteria were detected in the bladder lumen. Abbreviations. B = bladder, K = kidney, CI = competitive index. Bars represent mean (**A–E**), geometric mean (**F, H**), and median (**G**). *p<0.05, **p<0.01, ***p<0.001, ****p<0.0001 by Wilcoxon Signed Ranked test (**A–F**) or Mann Whitney U test (**G, H**). N = 10, 2 replicates (**A, G, H**); N = 11, 2 replicates (**B, E**); N = 16, 3 replictates (**C**); N = 18, 3 replicates (**D**); N = 20 mice, 4 replicates (**F, G**); N = 15, 3 replicates, (**H**); N = 4, 2 replicates (**I**). All replicates are biological.

DOI: https://doi.org/10.7554/eLife.31662.014

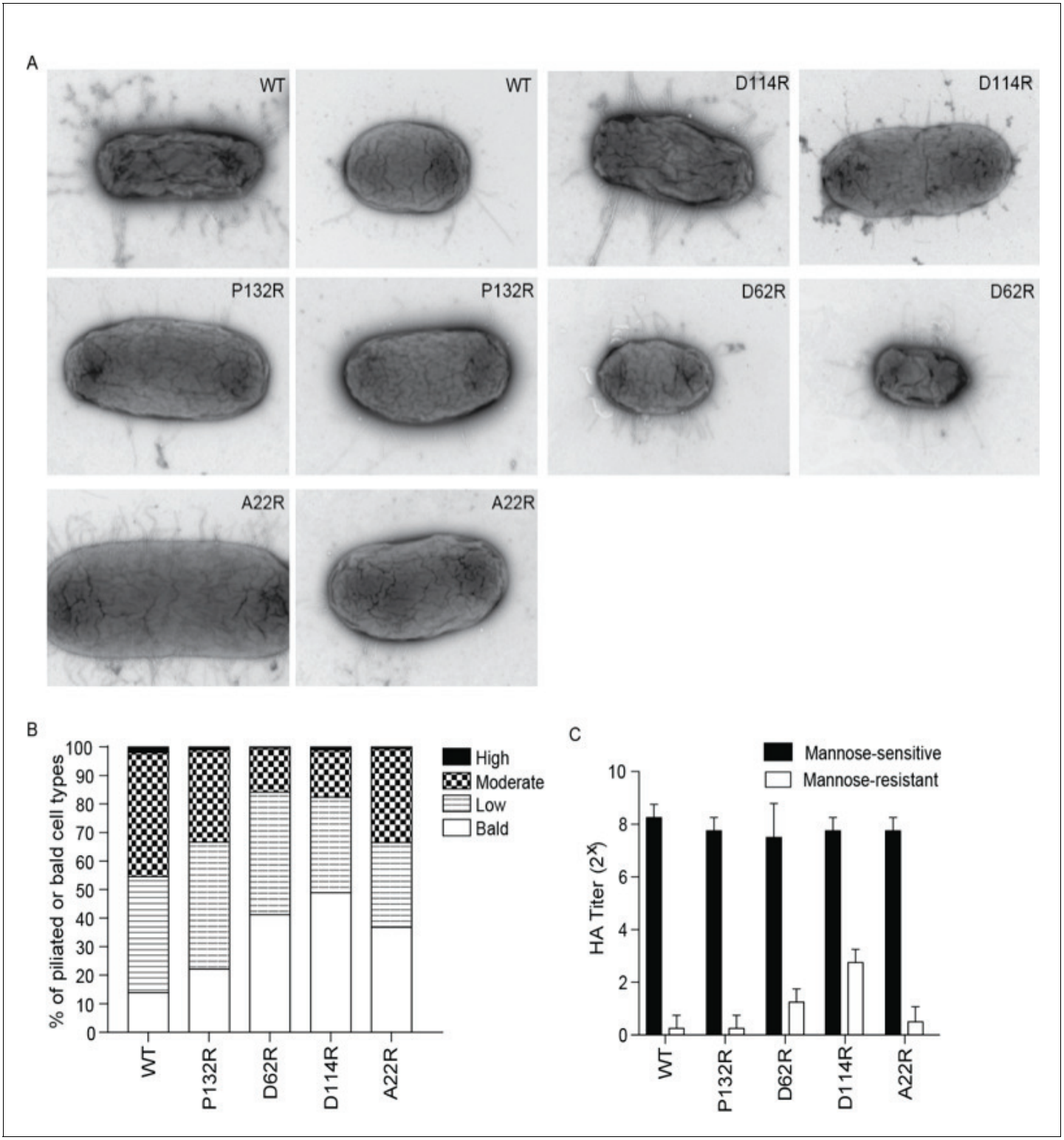

Figure 5—figure supplement 1. Chromosomally integrated point mutations in *fimA* gene do not prevent the expression or function of type 1 pili in vitro. (**A**) Representative negative stain EM images of UTI89 strains producing WT FimA or one of the indicated mutant variants. (**B**) Percentage of bald, lowly-, moderately-, and highly-piliated cells in the different UTI89 populations. (**C**) The relative ability of the WT strain and each mutant to bind and agglutinate guinea pig red blood cells as assessed by hemagglutination titer analysis. Abbreviations: HA = hemagglutination assay. Bars represent mean ±SD (**C**). N = 600 cell counted per mutant, two biological replicates (**B**); N = 4 biological replicates with two technical replicates each (**C**).
DOI: https://doi.org/10.7554/eLife.31662.015

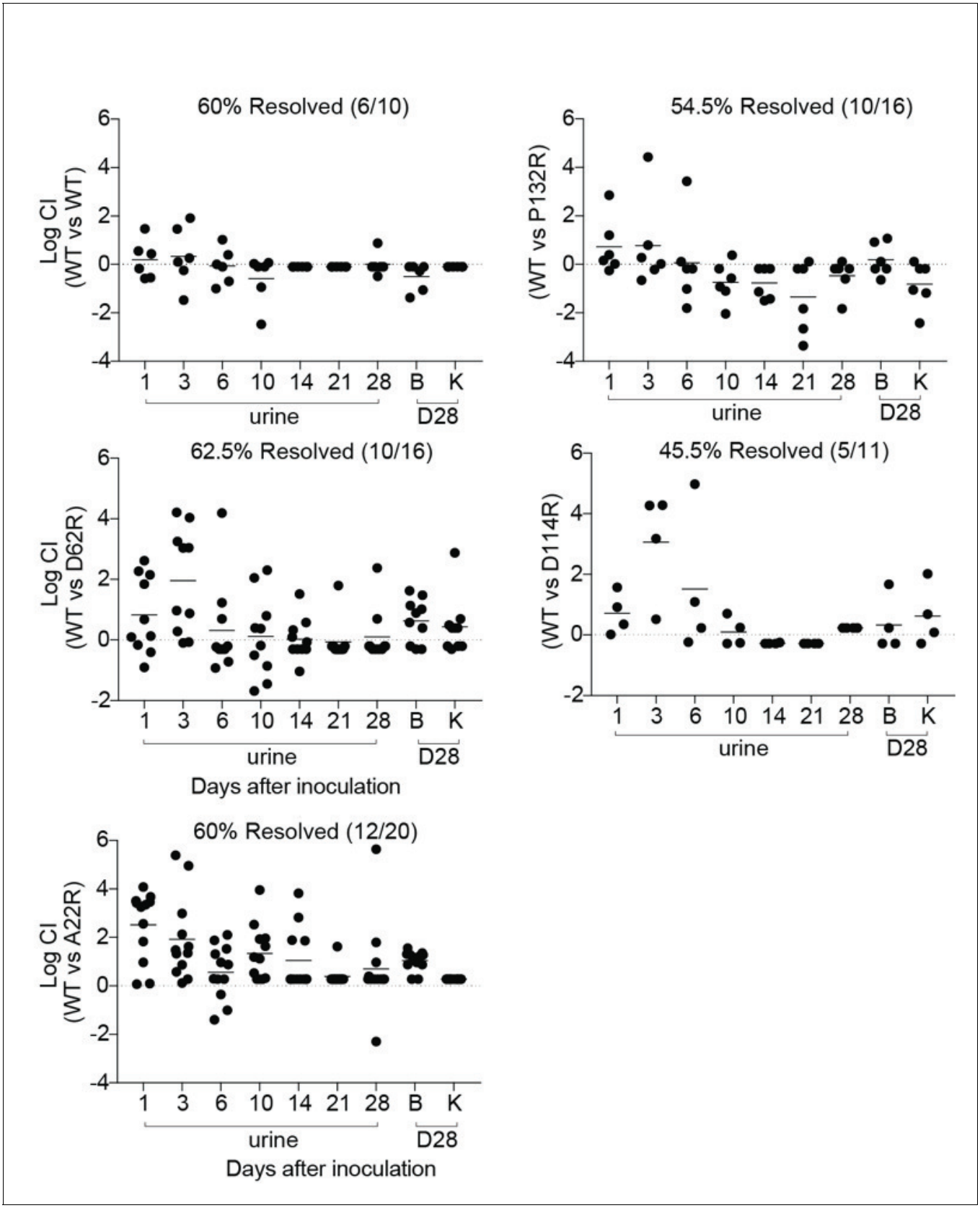

Figure 5—figure supplement 2. CFU titers for mice that resolved competitive bladder infections shown in ***Figure 5***. C3H/HeN mice were concurrently colonized, via transurethral inoculation, with 1×10^8 CFU of wildtype (WT) UTI89 and one of 4 isogenic UTI89 strains containing point mutations in *fimA*.

Figure 5—figure supplement 2 continued on next page

Figure 5—figure supplement 2 continued

The resolution of infection in mice was determine by longitudinal urinalysis and examination of UTI89 titers in bladders and kidneys at time of sacrifice (28 dpi). The mice that resolved infection by both strains (percentage shown above each graph) are shown here. Chronically infected mice are shown in ***Figure 5***. Abbreviations. B = bladder, K = kidney, CI = competitive index. Bars represent mean values.

DOI: https://doi.org/10.7554/eLife.31662.016

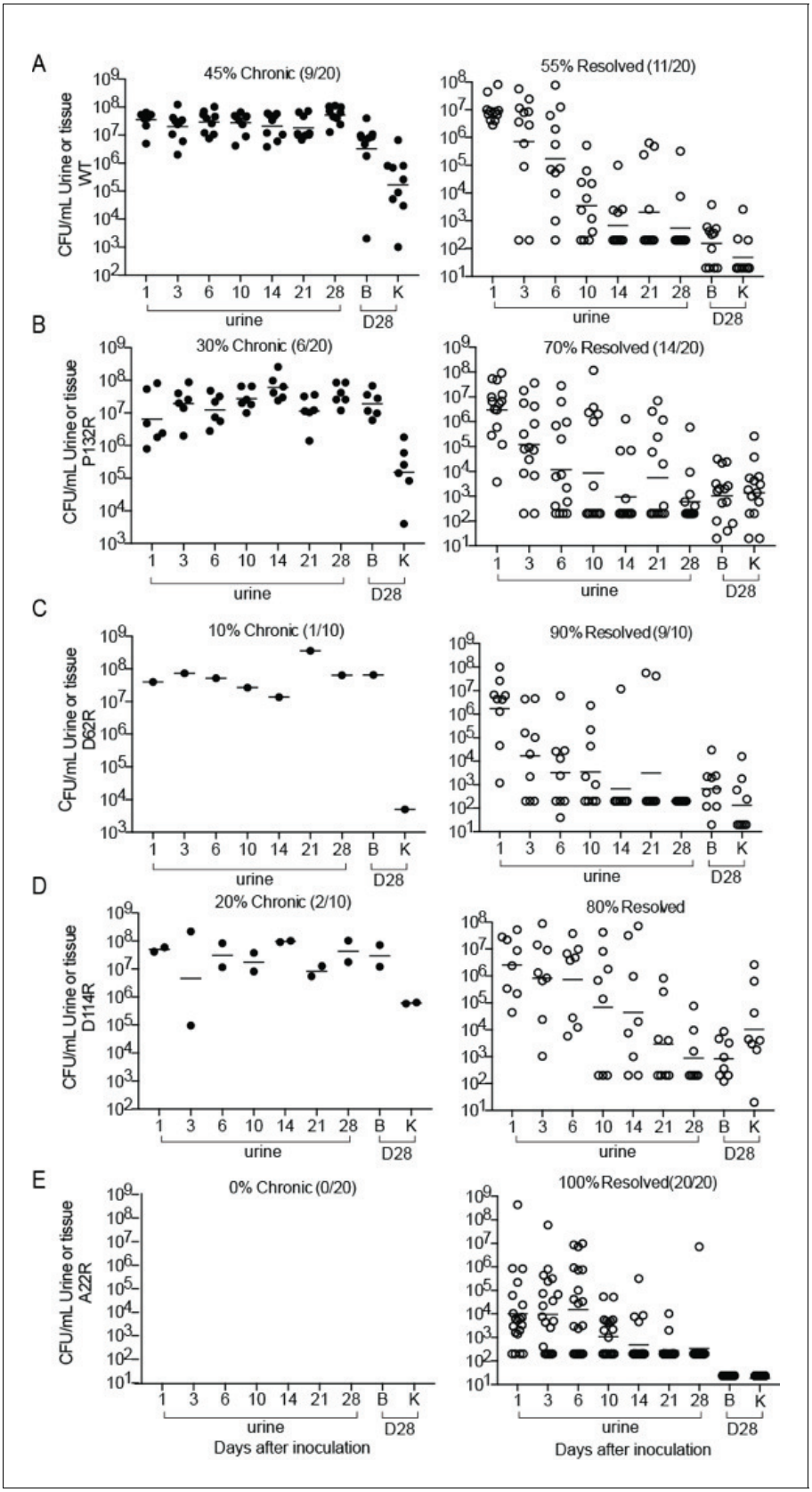

Figure 5—figure supplement 3. CFU titers for mice that developed chronic UTI or resolved infection in single bladder infections shown in Figure 5. (**A–E**) C3H/HeN mice were singly colonized, via transurethal inoculation, with 1×10^8 CFU of wildtype (WT) UTI89 or one of 4 isogenic UTI89 strains

Figure 5—figure supplement 3 continued on next page

Figure 5—figure supplement 3 continued

containing point mutations in *fimA*. The status of infection (mice that were chronically infected or those that resolved infection) was determine by longitudinal urinalysis and examination of UTI89 titers in bladders and kidneys at time of sacrifice (28 dpi). Mice that developed chronic infection are shown on the left while those that resolved infection are shown on the right. Percentages of each outcome are given above each graph. Abbreviations. B = bladder, K = kidney. Bars represent geometric mean.

DOI: https://doi.org/10.7554/eLife.31662.017

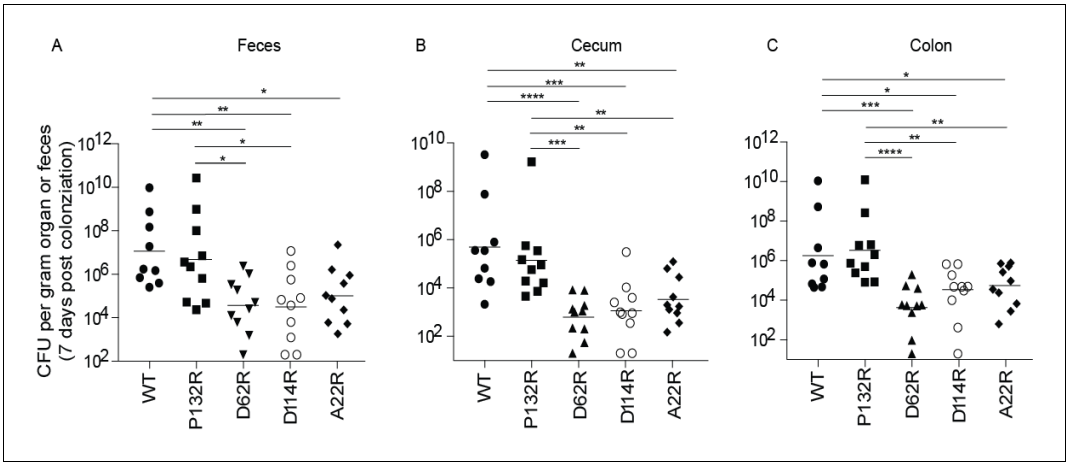

Figure 6. Mutations in FimA alter the ability of UTI89 to colonize the intestine. C3H/HeN mice were orally gavaged with streptomycin, to disrupt colonization resistance, and one day later orally gavaged with 1×10^8 CFU of WT UTI89 or one of 4 isogenic UTI89 strains with point mutations in *fimA*. The burden of each FimA mutant was determined via CFU counting in were determined the feces, cecum, or colon of mice at 7 days post colonization. Bars represent geometric mean. *p<0.05, **p<0.01, ***p<0.001, ****p<0.0001 by Mann Whitney U test. N = 10, 2 biological replicates.
DOI: https://doi.org/10.7554/eLife.31662.018